

# Solid-state welded interface characterization for boron-doped Ni<sub>3</sub>Al – Ti-6Al-4V couple and its comparison to Ni<sub>3</sub>Al – AISI 304 stainless steel couple

M. H. Kelestemur\*

*Melikşah University, Faculty of Engineering and Architecture, Department of Mechanical Engineering,  
Mevlana Mahallesi, Aksu Sokak No. 2, 38280 Talas, Kayseri, Turkey*

Received 27 April 2013, received in revised form 24 May 2013, accepted 23 October 2013

## Abstract

In this study, solid-state welding of boron-doped Ni<sub>3</sub>Al with Ti-6Al-4V was carried out to determine the nature of the interface species and bonding. The interface was examined with SEM, EDS, and micro-hardness tests. Interface stress distribution induced due to different thermal expansion properties was studied with ANSYS modeling. Due to eutectic transformation phenomenon occurring at the interface of boron-doped Ni<sub>3</sub>Al with Ti-6Al-4V couple, a brittle dendritic structure formed and the mismatched thermal expansion properties of materials led to crack formation at the welding zone. Also, a comparison of the interface zones for boron-doped Ni<sub>3</sub>Al with Ti-6Al-4V and boron-doped Ni<sub>3</sub>Al with AISI 304 stainless steel was provided to demonstrate different interface characteristics.

**Key words:** solid-state welding, boron-doped Ni<sub>3</sub>Al, Ti-6Al-4V, AISI 304 stainless steel, intermetallic alloy, Kirkandall effect

## 1. Introduction

Boron-doped Ni<sub>3</sub>Al intermetallic materials possess high temperature strength and hardness, excellent oxidation resistance, and adequate ductility; therefore, they have been used as high temperature structural materials (such as for aircraft gas turbines, combustor liners, high temperature discs, turbine vanes, turbine blades, etc.) and have been attracting significant interest for a few decades [1–6]. The widespread use of boron-doped Ni<sub>3</sub>Al with other numerous materials (such as Al<sub>2</sub>O<sub>3</sub>, W, AISI 304 stainless steel, TiB<sub>2</sub>, BN, etc.) in the form of laminated metal composites, clad metal composites, powder coated materials, etc. demands that boron-doped Ni<sub>3</sub>Al is properly joined (or welded) to other industrial materials [4, 5, 7–9]. Studying interfaces between boron-doped Ni<sub>3</sub>Al and other materials is critical to obtain a welding zone that is free of cracks and damages.

The amount of published literature regarding boron-doped Ni<sub>3</sub>Al material and its interaction with other materials is very scarce. Authors of this study

were aiming not only to study intermetallic interface formations as a metallurgical phenomenon and demonstrate how it affects the bonding at the welding zone, but also to validate that special care needs to be given to Ni<sub>3</sub>Al or other similar intermetallic materials during the solid-state or any other kind of welding processes. In this study, the authors explored the solid-state welding of boron-doped Ni<sub>3</sub>Al and Ti-6Al-4V and characterized the interface, and to our knowledge this is the first study that provides detailed information for these materials.

## 2. Materials and methods

Boron-doped Ni<sub>3</sub>Al, Ti-6Al-4V, and AISI 304 austenitic stainless samples were purchased from the commercial vendors and were used in the experiments in the as received form. Boron-doped Ni<sub>3</sub>Al, Ti-6Al-4V, and AISI 304 austenitic stainless samples were cut in the dimensions of 10 × 10 mm<sup>2</sup>. Sample surfaces were subjected to mirror-like polishing by using the

\*Corresponding author: tel.: +90 533 564 5008; fax: +90 352 207 7249; e-mail address: [hkelestemur@meliksah.edu.tr](mailto:hkelestemur@meliksah.edu.tr)

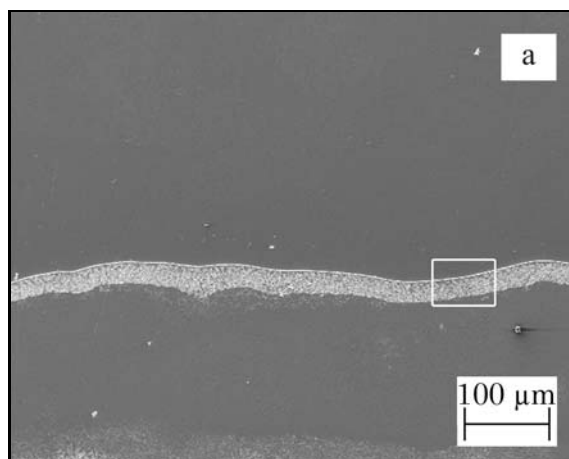


Fig. 1a. SEM images for the boron-doped Ni<sub>3</sub>Al – Ti-6Al-4V interface.

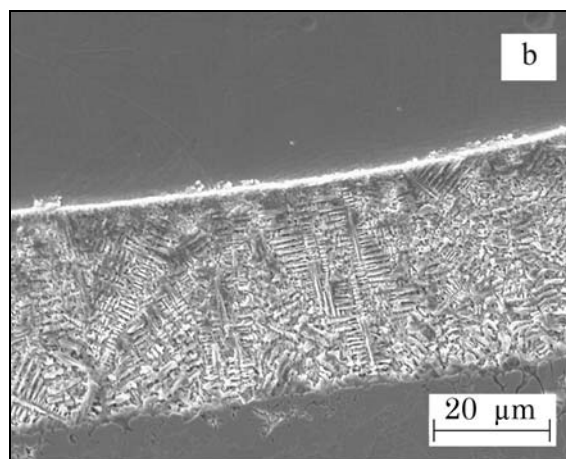


Fig. 1b. Enlarged interface section of Fig.1a to show the dendritic microstructure.

conventional metallographic polishing steps. After the polishing steps, samples were cleaned with ethyl alcohol before the welding process to remove the organic contaminants (such as grease, etc.). The welding was done with an AC type resistance spot welder and the welding temperature was estimated to be around 850 °C at the interface zone. The dwell time was set to 10 seconds and the compressive pressure was set to 6 MPa. For examination of the formed microstructures at the interfaces, HNO<sub>3</sub> + H<sub>2</sub>SO<sub>4</sub> + H<sub>2</sub>O (1:1:1 by volume) and 50% HCl + 50% H<sub>2</sub>O (by volume) solutions were used as the etching agents. HNO<sub>3</sub> + H<sub>2</sub>SO<sub>4</sub> + H<sub>2</sub>O solution was applied to the boron-doped Ni<sub>3</sub>Al side and 50% HCl + 50% H<sub>2</sub>O solution was applied to Ti-6Al-4V and AISI 304 sides. The major reason for the chemical etching was to improve the clarity of the images by intentionally forming certain physical irregularities on the samples surfaces. During the etching process, special care was given to make sure the etching solution does not contact with the interface zone. Micro-structural and EDS examinations were done with the Leica Light Microscope and Leo 440 Scanning Electron Microscope Instruments. Micro-hardness measurements were performed on the welding zone by using the Anton Paar and Paar Physica MHT-10 brand Micro-Hardness Tester. 10-g load was used during the micro-hardness measurements. The interface zone elasto-plastic analysis was modeled with the ANSYS modeling software package.

### 3. Results and discussion

#### 3.1. Boron-doped Ni<sub>3</sub>Al – Ti-6Al-4V couple

SEM was used to determine the microstructural properties of the welding zone (Fig. 1). EDS in conjunction with binary/ternary alloy phase diagrams

Table 1. The possible phase formations at the welding zone (or interface) of boron-doped Ni<sub>3</sub>Al – Ti-6Al-4V couple. The first column represents the distance and distance values with (-) sign show the boron-doped Ni<sub>3</sub>Al side. The interface scanned from boron-doped Ni<sub>3</sub>Al to Ti-6Al-4V side

Distance (μm)	Temperature (°C)	Possible phases
-160	800	$\gamma + \gamma'$
-140	800	$H + \gamma' + \eta$
-120	800	$\beta_2 + H + \eta$
-100	800	$NiTi_2 + H + \beta_2$
-80	800	$NiTi_2 + H + \beta_2$
-60	800	$\beta_2 + H + \eta$
-40	800	$NiTi_2 + H + \beta_2$
-20	800	$\xi + H + NiTi_2$

was used to determine the phase characteristics and possible phases of the interface species (Table 1, [10]). In Fig. 1a, the light (or white) colored region shows the interface, the top and bottom sections are comprised of Ti-6Al-4V and boron-doped Ni<sub>3</sub>Al, respectively. The close-up (enlarged) image for the welding zone, given in Fig. 1b, which is taken from intersection of dashed line, shows that the interface had a dendritic structure. Binary and ternary alloy phase diagrams for Ti, Ni, and Al elements show that with approximately 25% Ni concentrations, formed interface species will possess eutectic properties with low melting point values [10]. EDS results showed that the interface composition was comprised of the following percentages: 25.45% Ni, 11.28% Al, and 63.27% Ti. Since the formed interface had approximately 25% Ni in the composition, welding zone most likely experienced a melting step due to eutectic formulation and hence, formed a dendritic structure.

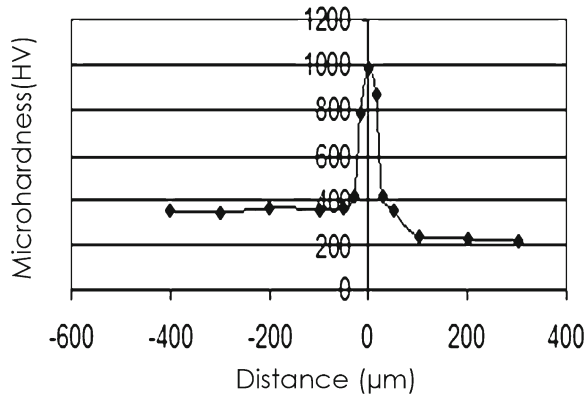


Fig. 2. Concentration profiles for interface species (*via* EDS analysis) for a boron-doped  $\text{Ni}_3\text{Al}$  -  $\text{Ti-6Al-4V}$  welded sample.

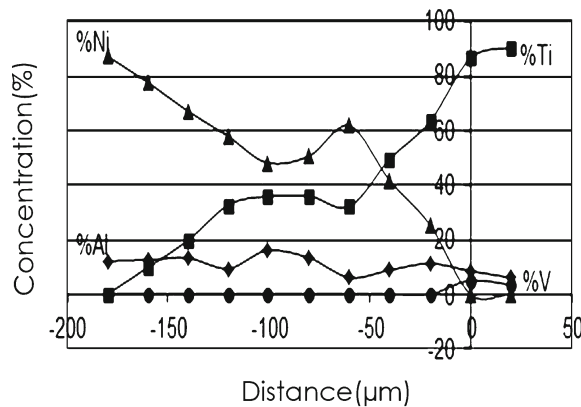


Fig. 3. Micro-hardness measurement for a boron-doped  $\text{Ni}_3\text{Al}$  -  $\text{Ti-6Al-4V}$  welded sample.

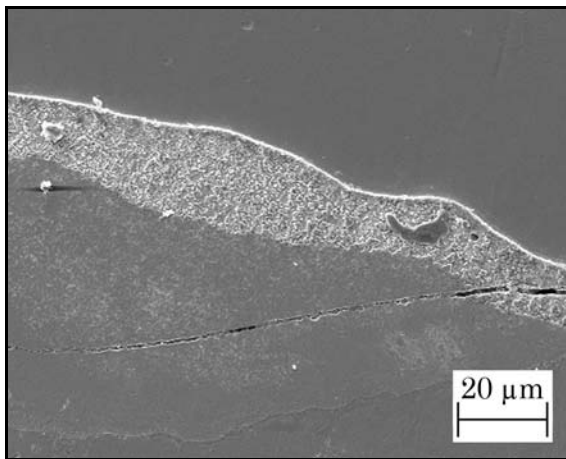


Fig. 4. SEM image indicating the macro- and micro-cracks at the boron-doped  $\text{Ni}_3\text{Al}$  -  $\text{Ti-6Al-4V}$  interface.

Atomic concentration profiles for interface species were determined using the protocol given by Aleman et al. [11] and they are given in Fig. 2. A typical

Kirkandall effect was observed at the interface. Interface micro-hardness characterization results are given in Fig. 3 and these results clearly indicate that intermetallic species formed at the interface increased the hardness significantly. Figure 4 shows the crack formation at the interface, which can be attributed to the hardness and brittleness of the interface and mismatched thermal expansion properties of the materials.

ANSYS modeling software was used to model the stress distribution and analyze the elasto-plastic properties of interface due to different thermal expansion properties of these materials. Finite Elements Method with 8-point iso-parametric elements (PLANE82) was used. Von Mises equivalent stress values were calculated between 500 and 1100 °C (100 °C incremental) to determine the stress distribution. The modeling results demonstrate that most of the stress was observed at the interface of contact points. Maximum stress vs. temperature curve demonstrates that there was a linear relationship between the maximum stress and temperature variables until up to 600 °C, and this linearity was not observed between 600 and 1100 °C. The linear relationship indicates that the interface demonstrated an elastic deformation and the non-linear relationship indicates the occurrence of both elastic and plastic deformations. Observing the cracks at the interface also validates the presence of plastic deformations.

### 3.2. Comparison of boron-doped $\text{Ni}_3\text{Al}$ - $\text{Ti-6Al-4V}$ to boron-doped $\text{Ni}_3\text{Al}$ - $\text{AISI 304}$ stainless steel

Results for the boron-doped  $\text{Ni}_3\text{Al}$  -  $\text{AISI 304}$  stainless steel couple was given in a prior publication that was published in the Materials Letters Journal [7] by the authors of this article.

The interface formed between boron-doped  $\text{Ni}_3\text{Al}$  -  $\text{AISI 304}$  stainless steel couple had a much lower micro-hardness value at the interface (approximately 480 HV) than the boron-doped  $\text{Ni}_3\text{Al}$  -  $\text{Ti-6Al-4V}$  couple (approximately 1000 HV). Since boron-doped  $\text{Ni}_3\text{Al}$  and  $\text{AISI 304}$  did not generate eutectic interface species with low melting point that can form a brittle microstructure and these materials had similar (or matched) thermal expansion properties to each other, the interface formed was free of macro- and micro-cracks. On the other hand, the interface formed between boron-doped  $\text{Ni}_3\text{Al}$  and  $\text{Ti-6Al-4V}$  had macro- and micro-cracks due to metallurgical properties of the generated interface species and mismatched thermal expansion properties.

## 4. Conclusions

Solid-state welding behavior of boron-doped  $\text{Ni}_3\text{Al}$

and Ti-6Al-4V couple was investigated and characterized. SEM, EDS, micro-hardness testing, and ANSYS modeling results indicate that solid-state welding of these two materials produces the welding zone with eutectic interface species that has low melting point values. Generating eutectic species forces the interface to experience a melting phenomenon which results in a dendritic microstructure with embrittlement issues. The welding zone for boron-doped Ni<sub>3</sub>Al – Ti-6Al-4V demonstrated macro- and micro-crack due to mismatched thermal expansion, dendritic and brittle interface species' properties. To successfully achieve solid-state welding of such materials, it is vital to explore different welding approaches such as adding another metallic layer or investigating different welding parameters.

### Acknowledgements

One of the contributors of this article was Sukrü Yildirim, who was working for Fırat University, School of Engineering, Metallurgical and Materials Department, Elazığ, Turkey, and he passed away in October 10, 2005. The main objective of this publication was to honor his work and make it accessible to the scientific community. The author thanks Mehmet Kesmez for his helpful consultation during the reorganizing the study.

### References

- [1] Gibbons, J. H.: *Strategic Materials: Technologies to Reduce U.S. Import Vulnerability*. Washington, D.C., U.S. Congress, Office of Technology Assessment, OTA-ITE-248, May 1985.
- [2] Aoki, K., Izumi, O.: *Nippon Kinzaku Gakkaisshi*, 43, 1979, p. 1190.
- [3] Villars, V.: *Intermetallic Compounds*. Eds.: Westbrook, J. H., Fleischer, D. New York, John Wiley and Sons 1995.
- [4] Yoo, M. H., Sass, S. L., Fu, C. L., Mills, M. J., Dimiduk, D. M., George, E. P.: *Acta Mater.*, 41, 1993, p. 987.
- [5] Ishikawa, A., Aoki, K., Masumoto, T.: In: *Proc. of 6th Materials Research Society Symposium*, vol. 364. Eds.: Baker, I., Hanada, S., Horton, J., Noebe, R. D., Schwartz, D. S. Pittsburgh, Materials Research Society 1995, p. 837.
- [6] Cahn, R. W.: *Load-Bearing Ordered Intermetallic Compounds – Historical View*, MRS Bulletin, 1991, p. 18.
- [7] Yildirim, S., Kelestemur, M. H.: *Mater Lett.*, 59, 2005, p. 1134. [doi:10.1016/j.matlet.2004.08.042](https://doi.org/10.1016/j.matlet.2004.08.042)
- [8] Goto, T., Cheng, Y., Fu, Z., Zhang, L.: *Adv Mater Res.*, 66, 2009, p. 194.
- [9] Chou, T. C.: *Appl Phys Lett.*, 53, 1988, p. 1500. [doi:10.1063/1.100467](https://doi.org/10.1063/1.100467)
- [10] *ASM Handbook, Alloy Phase Diagrams*, Vol. 3, 1992.
- [11] Gutiérrez, A. I., Urcola, J. J.: *Scripta Mater*, 36, 1997, p. 509. [doi:10.1016/S1359-6462\(96\)00414-9](https://doi.org/10.1016/S1359-6462(96)00414-9)